Side Chain Redistribution as a Strategy to Boost Organic Electrochemical Transistor Performance and Stability

Maximilian Moser,* Tania Cecilia Hidalgo, Jokubas Surgailis, Johannes Gladisch, Sarbani Ghosh, Rajendar Sheelamanthula, Quentin Thiburce, Alexander Giovannitti, Alberto Salleo, Nicola Gasparini, Andrew Wadsworth, Igor Zozoulenko, Magnus Berggren, Eleni Stavrinidou, Sahika Inal, and Iain McCulloch*

A series of glycolated polythiophenes for use in organic electrochemical transistors (OECTs) is designed and synthesized, differing in the distribution of their ethylene glycol chains that are tethered to the conjugated backbone. While side chain redistribution does not have a significant impact on the optoelectronic properties of the polymers, this molecular engineering strategy strongly impacts the water uptake achieved in the polymers. By careful optimization of the water uptake in the polymer films, OECTs with unprecedented steady-state performances in terms of [μC^*] and current retentions up to 98% over 700 electrochemical switching cycles are developed.

Organic electrochemical transistors (OECTs) are bioelectronic devices that have received considerable recent interest due to their ability to track biological activity.[1–10] Among the classes of channel materials developed for OECTs, ethylene glycol (EG)-functionalized organic semiconductors are particularly attractive due to: i) their high OECT performance, rivalling that of poly(3,4-ethylenedioxythiophene) (PEDOT) analog benchmarks,[11–13] ii) the general lack of post-processing treatments and solvent additives required to achieve maximum OECT performance,[14,15] iii) their facile synthetic tunability,[11,16–18] iv) the

absence of any insulating polyelectrolyte component improving their volumetric capacitance, and v) their excellent compatibility with enzymes allowing for direct detection of biologically relevant metabolites.[7,19]

Several molecular design strategies have been employed to boost the performance of glycolated semiconductors for OECTs, including: changing the EG chain length,[20] using mixed alkyl/EG solubilizing chains[17,21] and altering the aromatic moieties in the conjugated backbone.[4,11,12,18,22] The success of these strategies is typically evaluated by comparing the OECT steady-state performance, which is accomplished by assessing the maximum transconductance (g_m) that can be achieved in devices[23]

$$g_m = \mu C^* \frac{Wd}{L}(V_{TH} - V_G) \tag{1}$$

where μ is the electronic charge carrier mobility, C^* is the volumetric capacitance, W, d, and L are the channel width, depth,

M. Moser, Dr. N. Gasparini, Dr. A. Wadsworth
Department of Chemistry and Center for Plastic Electronics
Imperial College London
London W12 0BZ, UK
E-mail: maximilian.moser13@imperial.ac.uk

T. C. Hidalgo, J. Surgailis, Prof. S. Inal
Organic Bioelectronics Laboratory
Biological Sciences and Engineering Division
King Abdullah University of Science and Technology (KAUST)
Thuwal 23955-6900, Saudi Arabia

J. Gladisch, Dr. S. Ghosh, Prof. I. Zozoulenko, Prof. M. Berggren,
Prof. E. Stavrinidou
Laboratory of Organic Electronics
Department of Science and Technology
Linköping University
Norrköping SE-60174, Sweden

The ORCID identification number(s) for the author(s) of this article can be found under https://doi.org/10.1002/adma.202002748.

J. Gladisch, Prof. I. Zozoulenko, Prof. M. Berggren, Prof. E. Stavrinidou
Department of Science and Technology
Wallenberg Wood Science Center
Linköping University
Norrköping SE-60174, Sweden

Dr. R. Sheelamanthula, Prof. I. McCulloch
Physical Science and Engineering Division
King Abdullah University of Science and Technology (KAUST)
Thuwal 23955-6900, Saudi Arabia
E-mail: iain.mcculloch@kaust.edu.sa

Dr. Q. Thiburce, Dr. A. Giovannitti, Prof. A. Salleo
Department of Materials Science and Engineering
Stanford University
Stanford, CA 94305, USA

Prof. I. McCulloch
Department of Chemistry
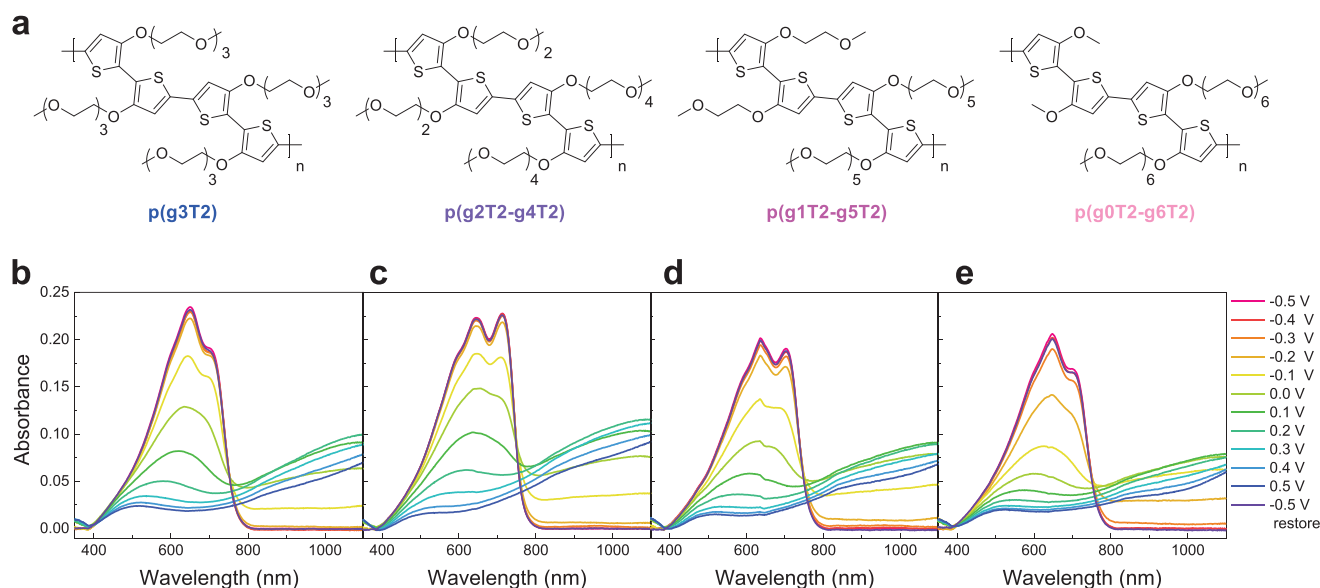University of Oxford
Oxford OX1 3TA, UK

Figure 1. a) Chemical structures of polymers investigated. Spectroelectrochemistry of b) p(g3T2), c) p(g2T2-g4T2), d) p(g1T2-g5T2), and e) p(g0T2-g6T2) employing a 0.1 M NaCl$_{(aq)}$ electrolyte.

and length, respectively, V_{Th} is the threshold voltage, and V_G is the gate voltage.

As highlighted in Equation (1), the g_m depends on both material ([μC^*]) and device geometry dependent terms (Wd/L). A more representative performance comparison of different channel materials is thus accomplished by comparison of [μC^*].[13] Currently, the highest [μC^*] recorded for glycolated semiconductors is 261 F cm^{-1} V^{-1} s^{-1} for p(g2T-TT),[12,13] while the highest [μC^*] reported for any OECT channel material is 490 F cm^{-1} V^{-1} s^{-1} for Crys-P.[15]

Although OECT steady-state performance is obviously of crucial importance, an equally significant but often overlooked parameter, is device stability, with few studies focusing on the operational stability of the materials during operation.[16,22,24,25] This aspect is however particularly relevant for the application of OECTs as ion and biomolecule sensors and implantable brain signal recorders.[5–7,9] Among the various high performance channel materials, the current benchmark, p(g2T-TT), has demonstrated devices retaining only 75% of their initial current ($I_D/I_{D,0}$) after ≈700 doping/dedoping cycles (2 h of constant electrochemical cycling), hence highlighting the need for more stable materials for the commercialization of OECT technologies.[12]

With these considerations in mind, we herein outline a new molecular design strategy, by which we successfully improved both device performance and operational stability. In fact, we report [μC^*] values of 522 and 496 F V^{-1} cm^{-1} s^{-1} and corresponding ($I_D/I_{D,0}$) retentions of 87% and 98% after ≈700 doping/dedoping cycles (2 h of constant electrochemical cycling) for two of our polymers.

The polymer series investigated was derived from the previously reported p(gT2) homopolymer (from here onwards referred to as p(g3T2)).[26,27] Next, the EG length on one bithiophene moiety was increased by one repeat unit and simultaneously decreased by one on the successive bithiophene moiety (from here onward referred to as "side chain redistribution"), affording the alternating diethylene-tetraethylene

glycol polymer, p(g2T2-g4T2). Further redistributions in the side chains led to the alternating monoethylene–pentaethylene glycol, p(g1T2-g5T2), and the alternating methoxy-hexaethylene glycol, p(g0T2-g6T2), polymers. The polymers' structures are shown in **Figure 1**a. Note that the average number of EG repeat units per polymer repeat unit remained constant across the series in this design strategy. An average of three EG units per thiophene ring was selected to ensure good polymer solubility. Moreover, we envisaged that an alkoxy substituent on each thiophene ring could be beneficial towards device stability as: i) the lone pair of electrons of the oxygen atom directly conjugated to the aromatic backbone can donate electron density via resonance, thus lowering the polymers' ionization potential (IP) and stabilizing the charged polymer species and ii) the added steric bulk from the substituent, should shield the conjugated backbone from interfering chemical species.

The synthesis of the polymers involved: i) transetherification of 3-methoxythiophene with the corresponding EG chain, ii) homocoupling of the resulting 3-substituted thiophene, and iii) functionalization of the bithiophene coupling partner to enable subsequent Stille crosscoupling polymerization. A detailed account of the synthetic procedures can be found in the Supporting Information.

The electrochemical properties of the polymers were characterized by cyclic voltammetry, UV–vis spectroscopy, and spectroelectrochemistry. Details regarding the experimental set-up are located in the Supporting Information. The polymers' onset of oxidation in organic ($E_{ox,org}$) and aqueous ($E_{ox,aq}$) media, IPs, maximum absorption wavelength in solution ($\lambda_{max,soln}$) and film ($\lambda_{max,film}$), and optical gap ($E_{g,opt}$) are summarized in **Table 1**. Figure S1 (Supporting Information) illustrates that each polymer can be electrochemically switched, reversibly, in organic and aqueous media. The presence of two cathodic peaks also indicates that the polymers can be oxidized twice within the given potential range, consistent with previous reports on glycolated polythiophenes.[18,27] As seen in Table 1 the

**ADVANCED
SCIENCE NEWS**

www.advancedsciencenews.com

**ADVANCED
MATERIALS**

www.advmat.de

Table 1. Polymers' optoelectronic properties.

Polymer	$E_{ox,org}$ [V][a]	$E_{ox,aq}$ [V][b]	IP [eV]	$\lambda_{max,soln}$ [nm][c]	$\lambda_{max,film}$ [nm][d]	$E_{g,opt}$ [eV][e]
p(g3T2)	−0.20	−0.18	4.46	577	641,−696	1.65
p(g2T2-g4T2)	−0.20	−0.17	4.46	581	642,−709	1.64
p(g1T2-g5T2)	−0.16	−0.24	4.50	586	636,−699	1.65
p(g0T2-g6T2)	−0.23	−0.30	4.43	591	654,−705	1.64

[a]0.1 M solution of TBA PF$_6$ in acetonitrile used as electrolyte; [b]0.1 M NaCl$_{(aq)}$ used as electrolyte; [c]Measured in chloroform; [d]$\lambda_{max,film}$ recorded while applying −0.5 V; [e]Calculated from the onset of absorption.

polymers' $E_{ox,org}$ and $E_{ox,aq}$ was −0.20 ± 0.10 V, showing that side chain redistribution had little effect on the polymers' electronic properties. This was further confirmed by UV–vis spectroscopy (Figure S2, Supporting Information), where no significant differences were found across the polymer series, both in solution and thin film. For each polymer, $\lambda_{max,film}$ was bathochromically shifted compared to its $\lambda_{max,soln}$. Moreover, in the solid state each polymer displayed 0–0 and 0–1 vibronic peaks of comparable magnitude, thus not only indicating increased molecular ordering, but also suggesting similar degrees of order in the solid state. This hypothesis was further reflected in the grazing-incidence wide-angle X-ray scattering (GIWAXS) data recorded for as-cast samples of the various polymers (Figure S3, Supporting Information), whereby each polymer preferentially assumed an edge-on orientation, while featuring three-orders of lamellar scattering and no significant π–π stacking.

The polymers' doping mechanism was investigated by spectroelectrochemistry.[28] No significant differences were observed when conducting the measurements in aqueous or organic media (Figure 1b–e and Figure S4, Supporting Information). As shown in Figure 1b–e and Figure S4 (Supporting Information), each polymer was partially doped under ambient conditions, requiring a negative potential to fully dedope the films. Progressively increasing the voltage to +0.2 V resulted in the gradual depression of the π–π* peak (highest occupied molecular orbital (HOMO)–lowest unoccupied molecular orbital (LUMO) transition) with the concomitant appearance of an absorption feature at ≈1050 nm, which was attributed to the polymers' polaron.[29] Further increasing the potential to +0.5 V decreased the intensity of this absorption feature which could be explained by the possible formation of an even longer wavelength absorbing feature, related to the formation of polaronic/bipolaronic species of the polymers.[29,30] Inversion of the potential to −0.5 V was employed to test the reversibility of the doping process. The optical signature of the polymers was fully restored in both media, indicating no polymer degradation when cycling the polymers within the given limits. The reversible and stable electrochemical charging of the films suggests that these polymers are ideal candidates as cathodes for energy applications[31] or electrochromic display applications, such as smart windows.[32]

Microscale OECTs were fabricated for each polymer. Full details of the OECT fabrication process can be found in the Supporting Information. Devices were operated using a 0.1 M NaCl$_{(aq)}$ electrolyte and an Ag/AgCl pellet as gate electrode.

As shown in **Figure 2**, all devices could be operated in enhancement mode with the devices' V_{Th} exactly mirroring the polymers' $E_{ox,aq}$ order. [μC^*] was calculated from Equation (1). To the best of our knowledge the [μC^*] for p(g2T2-g4T2) and p(g1T2-g5T2) are currently the highest reported for any OECT channel material.[13,15] Note that these [μC^*] values were obtained without any postprocessing treatments, often required for other high-performance channel materials.[14,15]

To better understand the performance difference across the polymers, we individually compared the results incurred for C^* and μ_{OECT}. C^* values were recorded with electrochemical impedance spectroscopy (EIS) at the V_G incurring the maximum g_m and fit to a $R_s(R_p//C)$ circuit.[12] A good fit between theoretical and experimental values was observed (Figure S5, Supporting Information). As seen from **Table 2** the C^* increased from 156 ± 1 F cm^{-3} for p(g3T2) to 187 ± 8 F cm^{-3} for p(g2T2-g4T2), while further side chain redistributions resulted in decreased C^* of 133 ± 3 and 74 ± 4 F cm^{-3} for p(g1T2-g5T2) and p(g0T2-g6T2), respectively. Given the absence of any differences in the anticipated doping levels of the polymers as suggested by spectroelectrochemistry, we conducted electrochemical quartz crystal microbalance with dissipation monitoring (EQCM-D) studies to investigate the swelling properties of the films and discuss the differing C^* of the polymers. EQCM-D was used to quantify the changes in mass and viscoelasticity from the influx of ions and water into the organic semiconductor.[20,26,33]

Figure S7 (Supporting Information) shows that each polymer displayed significant passive swelling upon electrolyte exposure in the absence of an applied bias, with the polymers swelling on average by 50 ± 15%. Passive swelling was attributed to the diffusion of ions and water into the films.[26] Subsequent doping of the polymers by applying +0.5 V increased their volume beyond their passively swollen state, which was attributed to the additional uptake of ions and water into the charged films.[26] Notably, significant differences in the active swelling were recorded, with p(g3T2), p(g2T2-g4T2), p(g1T2-g5T2), and p(g0T2-g6T2) incurring volume increases of 249%, 168%, 10%, and 4%, respectively. In line with previous studies, the polymers' decreased active swelling upon going from p(g2T2-g4T2) to p(g1T2-g5T2) and p(g0T2-g6T2) explained the corresponding decrease in C^* (Figure 2d).[20] Conversely, p(g3T2)'s smaller C^* compared to p(g2T2-g4T2) was attributed to p(g3T2)'s additional swelling not actually contributing to any additional anion uptake, but only water (Figure 2e).[20] From a mechanistic standpoint, we speculate that the difference in active swelling observed across our polymer series can be attributed to the different abilities of the individual EG-functionalized bithiophene units to take up and stabilize water molecules in their doped state. Specifically, our understanding is based on the idea that increasing the EG chain length on the individual bithiophene units increases their hydrophilicity and ability to take up and stabilize water molecules in their doped state. Consequently, we anticipate the 3,3′-dimethoxy-2,2′-bithiophene moiety (g0T2) to be the least able to stabilize injected water molecules, while progressively increasing the number of EG repeat units to one (g1T2), to two (g2T2), etc., leads to a progressively increased water molecule uptake. Nonetheless, there appears to be a nonlinear positive relationship between EG side chain length and water molecule uptake,
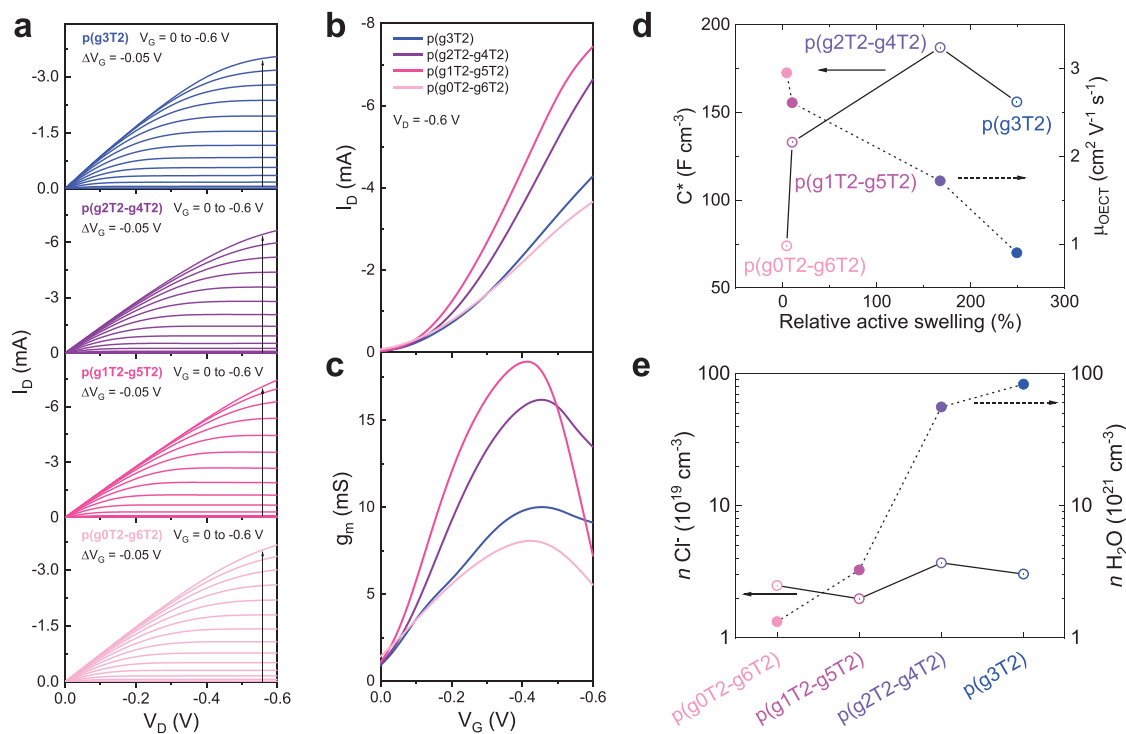
Figure 2. a) Output curves of the various polymers with a V_D sweep rate of 0.60 V s^{-1}. b) Transfer and c) corresponding transconductance curves of the various polymers with a V_G sweep rate of 0.60 V s^{-1}. d) Dependence of the polymers' C^* and μ_{OECT} on their active swelling. e) Concentration of chloride ions and water molecules taken up by polymers during in-situ doping using a 0.1 M NaCl$_{(aq)}$ electrolyte and applying +0.5 V.

with the relationship seemingly becoming weaker for any additional increases in the EG chain length after reaching three EG repeat units. This hypothesis corroborates the findings for an alternative polymer system, in which an initial doubling of the EG side chain content in the polymers under evaluation resulted in a ≈600% increase in the active swelling, while further doubling the EG chain content only resulted in a ≈50% increase in the active swelling.[20]

Given the strong dependence of the electronic transport on the swelling of materials,[33] the polymers' electronic mobility trend was also explained with EQCM-D findings. p(g3T2) featured the lowest mobility of 0.90 ± 0.10 cm^2 V^{-1} s^{-1}, while redistributing the EG chains increased μ_{OECT}, with p(g2T2-g4T2), p(g1T2-g5T2), and p(g0T2-g6T2) incurring mobilities of 1.72 ± 0.31, 2.61 ± 0.30, and 2.95 ± 0.37 cm^2 V^{-1} s^{-1}, respectively. Note how the increase closely correlates to the inverse of their active swelling, i.e., the polymers exhibiting the least swelling also attained the highest mobility (Figure 2d). A progressive

decrease in the hydration level of the glycolated semiconductors thus explains the increased mobility.[33]

From the chronoamperometry measurements conducted during our EQCM-D studies we were also able to calculate the diffusion coefficient of Cl$^-$ ions in our polymers (Figure S8, Supporting Information); full details of the calculations can be found in the Supporting Information. As shown in Figure S8 (Supporting Information), our results indicate that increasing the water uptake in polymer films enhanced ion diffusivity, thus agreeing with previous literature findings, which have shown faster ionic motion to occur in polymer films with a higher degree of hydration[34,35]

Lastly, we investigated the OECTs' operational stability (**Figure 3**) by switching the devices "on" and "off" for 5 s each and measuring the ($I_D/I_{D,0}$) over ≈700 doping/dedoping cycles (2 h of constant electrochemical cycling). While there is currently no standard defining the "on" state of the polymers, we herein suggest that the "on" state of the polymer should be the

Table 2. Steady-state OECT performance summary.

Polymer	d [nm]	g_m [mS]	$C^{*a)}$ [F cm^{-3}]	μ_{OECT}[b)] [cm^2 V^{-1} s^{-1}]	V_{Th} [V]	$[\mu C^*]$[c)] [F V^{-1} cm^{-1} s^{-1}]	On/off
p(g3T2)	75	8.9 ± 1.0	156 ± 1	0.90 ± 0.10	+0.03	161	10^5
p(g2T2-g4T2)	45	6.5 ± 1.6	187 ± 8	1.72 ± 0.31	+0.02	522	10^5
p(g1T2-g5T2)	65	10.2 ± 1.2	133 ± 3	2.61 ± 0.30	+0.10	496	10^5
p(g0T2-g6T2)	70	8.1 ± 1.0	74 ± 4	2.95 ± 0.37	+0.18	302	10^5

[a)]Values calculated from EIS curves fit to an $R_s(R_p//C)$ circuit; [b)]Calculated from the transistor saturation mobility using the respective C^* values; [c)]Calculated for the highest performing channel from the slope of g_m as a function of $(Wd/L)(V_{Th} - V_G)$.

ADVANCED
SCIENCE NEWS
www.advancedsciencenews.com

ADVANCED
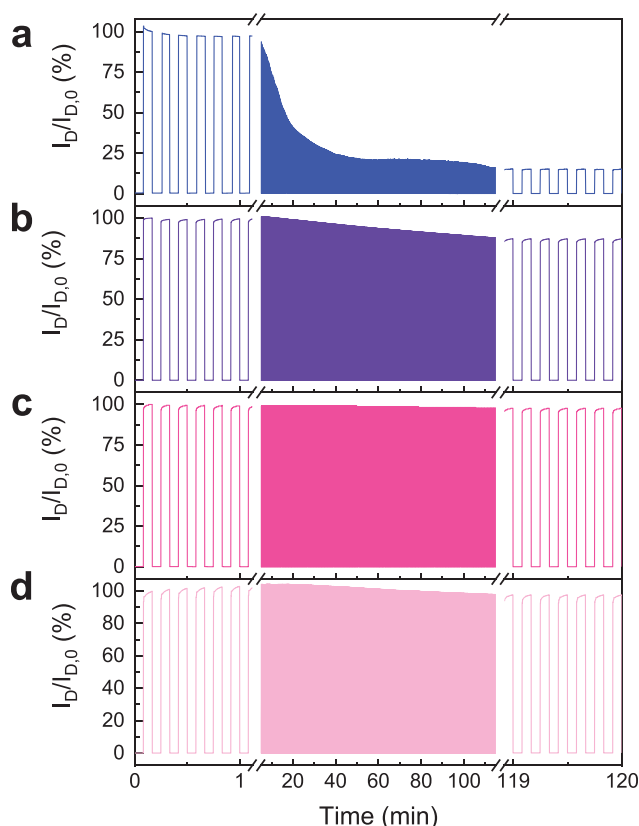**MATERIALS**
www.advmat.de

Figure 3. a–d) Operational stabilities of p(g3T2) (a), p(g2T2-g4T2) (b), p(g1T2-g5T2) (c), and p(g0T2-g6T2) (d) over 2 h continuous electrochemical cycling.

point affording the maximum transconductance. Consequently, the applied V_G and V_D potentials were those that incurred the maximum transconductance.

Despite the polymers' similar energy levels, their operational stability varied significantly (Figure 3). While p(g3T2) only retained 15% of its initial current, p(g2T2-g4T2), p(g1T2-g5T2), and p(g0T2-g6T2) showed much improved $I_D/I_{D,0}$ of 87%, 98%, and 98%, therefore also exceeding the 75% $I_D/I_{D,0}$ of the benchmark, p(g2T-TT).[12] Comparing the operational stability data with the swelling properties of the various polymers highlighted a strong inverse relationship between the polymers' degree of active swelling and their operational stabilities. Given the similar morphological features of the polymers in their dry as cast state and comparable degrees of passive swelling, we attributed the increased stability of the polymers with the lowest degree of active swelling to the significantly larger volumetric expansion during OECT cycling, which is likely to lead to increased morphological changes that are detrimental to OECT performance.

In conclusion, we have developed a molecular design strategy based on the redistribution of the pendant EG chains in a series of polythiophenes for OECT applications. While this strategy did not considerably impact the polymers' optoelectronic properties, it significantly impacted their swelling capabilities and consequently also their OECT steady-state performance and stability. Importantly, the development of p(g2T2-g4T2) and p(g1T2-g5T2), demonstrated unprecedented [μC^*] values of 496 and 522 F V^{-1} cm^{-1} s^{-1} and current retentions of 87% and 98%

over ≈700 electrochemical switching cycles, respectively, presenting a significant advancement in OECT channel materials.

Supporting Information

Supporting Information is available from the Wiley Online Library or from the author.

Conflict of Interest

The authors declare no conflict of interest.

[1] J. Rivnay, S. Inal, A. Salleo, R. M. Owens, M. Berggren, G. G. Malliaras, *Nat. Rev. Mater.* **2018**, *3*, 17086.

[2] X. Strakosas, M. Bongo, R. M. Owens, *J. Appl. Polym. Sci.* **2015**, *132*, 41735.

[3] R. M. Owens, G. G. Malliaras, *MRS Bull.* **2010**, *35*, 449.

[4] M. Moser, J. F. Ponder, A. Wadsworth, A. Giovannitti, I. McCulloch, *Adv. Funct. Mater.* **2019**, *29*, 1807033.

[5] D. Khodagholy, T. Doublet, P. Quilichini, M. Gurfinkel, P. Leleux, A. Ghestem, E. Ismailova, T. Hervé, S. Sanaur, C. Bernard, G. G. Malliaras, *Nat. Commun.* **2013**, *4*, 1575.

[6] A. M. Pappa, V. F. Curto, M. Braendlein, X. Strakosas, M. J. Donahue, M. Fiocchi, G. G. Malliaras, R. M. Owens, *Adv. Healthcare Mater.* **2016**, *5*, 2295.

[7] A. M. Pappa, D. Ohayon, A. Giovannitti, I. P. Maria, A. Savva, I. Uguz, J. Rivnay, I. McCulloch, R. M. Owens, S. Inal, *Sci. Adv.* **2018**, *4*, eaat0911.

[8] C. Liao, C. Mak, M. Zhang, H. L. W. Chan, F. Yan, *Adv. Mater.* **2015**, *27*, 676.

[9] J. Rivnay, M. Ramuz, P. Leleux, A. Hama, M. Huerta, R. M. Owens, *Appl. Phys. Lett.* **2015**, *106*, 043301.

[10] A. Campana, T. Cramer, D. T. Simon, M. Berggren, F. Biscarini, *Adv. Mater.* **2014**, *26*, 3874.

[11] C. B. Nielsen, A. Giovannitti, D. T. Sbircea, E. Bandiello, M. R. Niazi, D. A. Hanifi, M. Sessolo, A. Amassian, G. G. Malliaras, J. Rivnay, I. McCulloch, *J. Am. Chem. Soc.* **2016**, *138*, 10252.

[12] A. Giovannitti, D. T. Sbircea, S. Inal, C. B. Nielsen, E. Bandiello, D. A. Hanifi, M. Sessolo, G. G. Malliaras, I. McCulloch, J. Rivnay, *Proc. Natl. Acad. Sci. USA* **2016**, *113*, 12017.

[13] S. Inal, G. G. Malliaras, J. Rivnay, *Nat. Commun.* **2017**, *8*, 1767.

[14] J. Rivnay, S. Inal, B. A. Collins, M. Sessolo, E. Stavrinidou, X. Strakosas, C. Tassone, D. M. Delongchamp, G. G. Malliaras, *Nat. Commun.* **2016**, *7*, 11287.

[15] S. M. Kim, C. H. Kim, Y. Kim, N. Kim, W. J. Lee, E. H. Lee, D. Kim, S. Park, K. Lee, J. Rivnay, M. H. Yoon, *Nat. Commun.* **2018**, *9*, 3858.

[16] A. Giovannitti, C. B. Nielsen, D. T. Sbircea, S. Inal, M. Donahue, M. R. Niazi, D. A. Hanifi, A. Amassian, G. G. Malliaras, J. Rivnay, I. McCulloch, *Nat. Commun.* **2016**, *7*, 13066.

[17] Y. Wang, E. Zeglio, H. Liao, J. Xu, F. Liu, Z. Li, I. P. Maria, D. Mawad, A. Herland, I. Mcculloch, W. Yue, *Chem. Mater.* **2019**, *31*, 9797.

[18] L. R. Savagian, A. M. Österholm, J. F. Ponder, K. J. Barth, J. Rivnay, J. R. Reynolds, *Adv. Mater.* **2018**, *30*, 1804647.

[19] D. Ohayon, G. Nikiforidis, A. Savva, A. Giugni, S. Wustoni, T. Palanisamy, X. Chen, I. P. Maria, E. Di Fabrizio, P. M. F. J. Costa, I. McCulloch, S. Inal, *Nat. Mater.* **2020**, *19*, 456.

[20] A. Savva, R. Hallani, C. Cendra, J. Surgailis, T. C. Hidalgo, S. Wustoni, R. Sheelamanthula, X. Chen, M. Kirkus, A. Giovannitti, A. Salleo, I. McCulloch, S. Inal, *Adv. Funct. Mater.* **2020**, *30*, 1907657.

[21] A. Giovannitti, I. P. Maria, D. Hanifi, M. J. Donahue, D. Bryant, K. J. Barth, B. E. Makdah, A. Savva, D. Moia, M. Zetek, P. R. F. Barnes, O. G. Reid, S. Inal, G. Rumbles, G. G. Malliaras, J. Nelson, J. Rivnay, I. McCulloch, *Chem. Mater.* **2018**, *30*, 2945.

[22] A. Giovannitti, R. B. Rashid, Q. Thiburce, B. D. Paulsen, C. Cendra, K. Thorley, D. Moia, J. T. Mefford, D. Hanifi, D. Weiyuan, M. Moser, A. Salleo, J. Nelson, I. McCulloch, J. Rivnay, *Adv. Mater.* **2020**, *32*, 1908047.

[23] D. A. Bernards, G. G. Malliaras, *Adv. Funct. Mater.* **2007**, *17*, 3538.

[24] E. Zeglio, M. M. Schmidt, M. Thelakkat, R. Gabrielsson, N. Solin, O. Inganäs, *Chem. Mater.* **2017**, *29*, 4293.

[25] H. Sun, M. Vagin, S. Wang, X. Crispin, R. Forchheimer, M. Berggren, S. Fabiano, *Adv. Mater.* **2018**, *30*, 1704916.

[26] J. Gladisch, E. Stavrinidou, S. Ghosh, A. Giovannitti, M. Moser, I. Zozoulenko, I. McCulloch, M. Berggren, *Adv. Sci.* **2020**, *7*, 1901144.

[27] D. Moia, A. Giovannitti, A. A. Szumska, I. P. Maria, E. Rezasoltani, M. Sachs, M. Schnurr, P. R. F. Barnes, I. McCulloch, J. Nelson, *Energy Environ. Sci.* **2019**, *12*, 1349.

[28] S. Garreau, G. Louarn, J. P. Buisson, G. Froyer, S. Lefrant, *Macromolecules* **1999**, *32*, 6807.

[29] I. Zozoulenko, A. Singh, S. K. Singh, V. Gueskine, X. Crispin, M. Berggren, *ACS Appl. Polym. Mater.* **2019**, *1*, 83.

[30] S. Ghosh, V. Gueskine, M. Berggren, I. V. Zozoulenko, *J. Phys. Chem. C* **2019**, *123*, 15467.

[31] J. F. Mike, J. L. Lutkenhaus, *J. Polym. Sci., Part B: Polym. Phys.* **2013**, *51*, 468.

[32] R. J. Mortimer, A. L. Dyer, J. R. Reynolds, *Displays* **2006**, *27*, 2.

[33] A. Savva, C. Cendra, A. Giugni, B. Torre, J. Surgailis, D. Ohayon, A. Giovannitti, I. McCulloch, E. Di Fabrizio, A. Salleo, J. Rivnay, S. Inal, *Chem. Mater.* **2019**, *31*, 927.

[34] S. Inal, J. Rivnay, A. I. Hofmann, I. Uguz, M. Mumtaz, D. Katsigiannopoulos, C. Brochon, E. Cloutet, G. Hadziioannou, G. G. Malliaras, *J. Polym. Sci., Part B: Polym. Phys.* **2016**, *54*, 147.

[35] E. Stavrinidou, P. Leleux, H. Rajaona, D. Khodagholy, J. Rivnay, M. Lindau, S. Sanaur, G. G. Malliaras, *Adv. Mater.* **2013**, *25*, 4488.